*Inorg. Chem.* **2009**, *48*, 4165−4170

Inorganic Chemistry
Article

# Symmetry-Dependent Strong Reduction of the Spin Exchange Interactions in $Cs_2CuCl_4$ by the 6p Orbitals of $Cs^+$ Ions

**Changhoon Lee,[†] Jinhee Kang,[†,‡] Kee Hag Lee,[*,‡] and Myung-Hwan Whangbo[*,†]**

*Department of Chemistry, North Carolina State University, Raleigh, North Carolina 27695-8204, and Department of Chemistry, Nanoscale Science and Technology Institute, and BK21, Wonkwang University, Iksan 570-749, Korea*

Received December 18, 2008

Despite a three-dimensional arrangement of its $CuCl_4^{2-}$ ions, the magnetic properties of $Cs_2CuCl_4$ are explained by a two-dimensional frustrated triangular antiferromagnetic spin−lattice. The origin of this low-dimensional magnetism was explored by evaluating the spin exchange interactions of $A_2CuCl_4$ (A = Cs, Rb, K, Na) on the basis of first principles density functional calculations. The calculated spin exchange parameters agree with experiment only when the $Cs^+$ ions located between the $CuCl_4^{2-}$ ions are not neglected. The antiferromagnetic spin exchange interaction between adjacent $CuCl_4^{2-}$ ions is strongly reduced by the 6p orbitals of the intervening $Cs^+$ ions when the arrangement of the $CuCl_4^{2-}$ and $Cs^+$ ions has either mirror-plane or inversion symmetry. The observed magnetism of $Cs_2CuCl_4$ arises from this symmetry-dependent participation of the 6p orbitals of the $Cs^+$ ions in the spin exchange interactions between $CuCl_4^{2-}$ ions.

## 1. Introduction

Recently, $Cs_2CuCl_4$ has received much attention because of its unconventional magnetic properties such as magnetic-field induced Bose-Einstein condensation[1] and fractional spin quasiparticles.[2] The crystal structure of $Cs_2CuCl_4$ has a three-dimensional (3D) arrangement of $CuCl_4^{2-}$ ions separated by $Cs^+$ ions (Figure 1a).[3] The $CuCl_4^{2-}$ ion can be described as a distorted square plane or a distorted tetrahedron containing a $Cu^{2+}$ ($d^9$) ion. There are four different arrangements of nearest-neighbor $CuCl_4^{2-}$ ions so that $Cs_2CuCl_4$ has four Cu−Cl···Cl−Cu super-superexchange (SSE) paths ($J_1$−$J_4$) leading to 3D spin exchange interactions (Figure 1b). However, the explanation of the magnetic properties of $Cs_2CuCl_4$ requires the use of the two-dimensional (2D) triangular spin−lattice made up of the spin exchange $J_1$ and $J_2$ with the ratio $J_2/J_1 = 0.34$, parallel to the *bc*-plane (Figure 1c).[2,4] Here $J_1$ and $J_2$ are both antiferromagnetic (AFM), so that this lattice is spin frustrated.[5] This 2D triangular AFM spin−lattice, deduced from a fitting analysis of the spin wave dispersion relations obtained from neutron scattering experiments,[2,4] has not yet been confirmed by electronic structure calculations. Furthermore, the consideration of the geometrical parameters of the Cu−Cl···Cl−Cu SSE paths associated with $J_1$−$J_4$ (Table 1) lead one to predict a different spin−lattice for $Cs_2CuCl_4$. Figure 2 shows the arrangement of the $CuCl_4^{2-}$ and $Cs^+$ ions associated with each of the SSE interactions $J_1$−$J_4$. Several interatomic distances associated with these interactions are summarized in Table 1. In general, an SSE interaction involving the path M−L···L−M (M = transition metal, L = main group ligand) becomes stronger with decreasing the L···L contact distance.[6] Thus, according to the Cl···Cl distances of Table 1, $J_1$ and $J_3$ should be two dominant interactions with $J_1$ stronger than $J_3$. The resulting spin−lattice is a frustrated two-leg spin ladder (Figure 1d), which is quite different from the observed 2D triangular AFM spin−lattice.

* To whom correspondence should be addressed. E-mail: mike_whangbo@ncsu.edu.
† North Carolina State University.
‡ Wonkwang University.

(1) Radu, T.; Wilhelm, H.; Yushankhai, V.; Kovrizhin, D.; Coldea, R.; Tylczynski, Z.; Lühmann, T.; Steglich, F. *Phys. Rev. Lett.* **2005**, *95*, 127202.
(2) Coldea, R.; Tennant, D. A.; Tsvelik, A. M.; Tylczynski, Z. *Phys. Rev. Lett.* **2001**, *86*, 1335.
(3) (a) McGinnety, J. A. *J. Am. Chem. Soc.* **1972**, *94*, 8406. (b) Bailleul, S.; Svoronos, D.; Porcher, P.; Tomas, A. *C. R. Acad. Sci. Ser 2* **1991**, *313*, 1149. (c) Xu, Y.; Carlson, S.; Söderberg, K.; Norrestam, R. *J. Solid State. Chem.* **2000**, *153*, 212.
(4) Coldea, R.; Tennant, D. A.; Habitch, K.; Smeibidl, P.; Wolters, C.; Tylczynski, Z. *Phys. Rev. Lett.* **2002**, *88*, 137203.
(5) (a) Greedan, J. E. *J. Mater. Chem.* **2001**, *11*, 37. (b) Dai, D.; Whangbo, M.-H. *J. Chem. Phys.* **2004**, *121*, 672.
(6) Whangbo, M.-H.; Koo, H.-J.; Dai, D. *J. Solid State Chem.* **2003**, *176*, 417.

10.1021/ic802412x CCC: $40.75 
Published on Web 03/27/2009

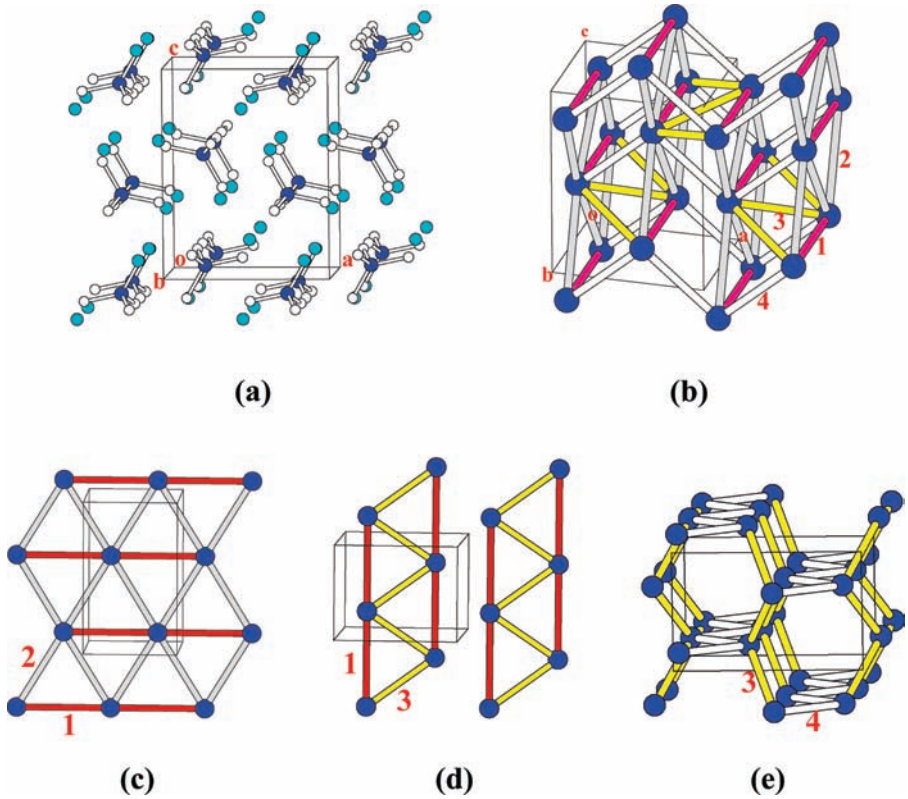


**Figure 1.** Schematic drawings showing the crystal structure and the spin exchange paths of $Cs_2CuCl_4$: (a) Arrangement of the $CuCl_4^{2-}$ and $Cs^+$ ions. (b) 3D arrangement of the four spin exchange paths $J_1-J_4$, where $J_1$, $J_2$, $J_3$, and $J_4$ are represented by the red, gray, yellow, and white cylinders, respectively. The numbers 1−4 in (b) refer to $J_1-J_4$, respectively. (c) 2D triangular net based on $J_1$ and $J_2$. (d) Two-leg spin ladder based on $J_1$ and $J_3$. (e) 3D lattice based on $J_3$ and $J_4$.

**Table 1.** Several Interatomic Distances (in Å) Associated with the Spin Exchange Paths $J_1-J_4$ in the RT and LT Crystal Structures of $Cs_2CuCl_4$

| | Cu···Cu | Cl···Cl | Cl···Cs |
|---|---|---|---|
| | | (a) RT Structure (ref 3a) | |
| $J_1$ | 7.609 | 3.634 | 3.460 (×2), 3.488 (×2), 3.636 (×2) |
| $J_2$ | 7.283 | 4.144 | 3.460, 3.483, 3.488, 3.518, 3.668 |
| $J_3$ | 6.802 | 4.076 (×2) | 3.599 (×2), 3.636 (×2) |
| $J_4$ | 6.417 | 4.103 (×2) | 3.630, 3.559, 3.668 (×2) |
| | | (b) Experimental (ref 3b) and Calculated LT Structures[a] | |
| $J_1$ | 7.607 | 3.623 | 3.889 (×2), 3.224 (×2), 3.635 (×2) |
| | 7.607 | 3.528 | 3.445 (×2), 3.495 (×2), 3.615 (×2) |
| $J_2$ | 7.276 | 4.145 | 3.889, 3.745, 3.224, 3.066, 3.676 |
| | 7.276 | 4.173 | 3.445, 3.537, 3.494, 3.514, 3.654 |
| $J_3$ | 6.809 | 4.079 (×2) | 3.587 (×2), 3.635 (×2) |
| | 6.815 | 4.050 (×2) | 3.550 (×2), 3.615 (×2) |
| $J_4$ | 6.419 | 4.104 (×2) | 3.629, 3.587, 3.676 (×2) |
| | 6.412 | 4.176 (×2) | 3.572, 3.550, 3.654 (×2) |

[a] For each entry, the values of the upper row refer to the experimental LT crystal structure, and those of the lower row to the calculated LT crystal structure.

In the present work, we examine the origin of the 2D triangular AFM spin−lattice by evaluating the spin exchange interactions of $Cs_2CuCl_4$ on the basis of first principles density functional theory (DFT) electronic structures calculations. The crystal structures of $Cs_2CuCl_4$ determined at room temperature (RT),[3a] at 0.3 K [hereafter referred to as the low-temperature (LT)],[3b] and under pressure[3c] are known. Our calculations were carried out for the RT and LT structures because they are relevant for the discussion of the magnetic properties of $Cs_2CuCl_4$. Our study reveals that the spin exchange between adjacent $CuCl_4^{2-}$ ions can be strongly reduced by the 6p orbitals of the intervening $Cs^+$ ions if the arrangement of the $CuCl_4^{2-}$ and $Cs^+$ ions has mirror-plane or inversion symmetry.

## 2. Spin Exchange Parameters from Cluster Calculations

We first evaluate the SSE parameters $J_1-J_4$ by performing DFT calculations for the four dimer clusters $(CuCl_4^{2-})_2$ representing these interactions by using the Gaussian 03 program package[7] with the B3LYP exchange-correlation

(7) Frish, M. J. et al. *Gaussian 03*, B.04; Gaussian, Inc.: Pittsburgh, PA, 2003.

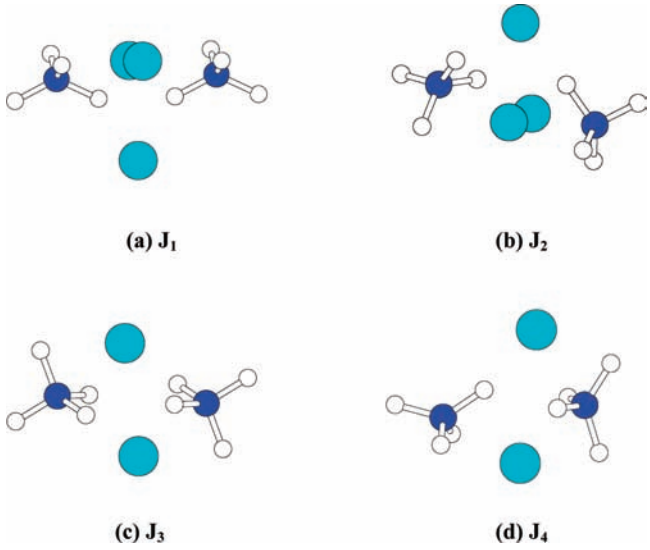


**Figure 2.** Arrangements of the two $CuCl_4^{2-}$ and the intervening $Cs^+$ ions associated with the spin exchange paths $J_1-J_4$.

**Table 2.** Spin Exchange Parameters $J_1/k_B-J_4/k_B$ (in K) of $A_2CuCl_4$ (A = Cs, Rb, K, Na) Determined from the GGA+U Calculations (with $U$ = 6 eV) for Their RT Structures and Those of $Cs_2CuCl_4$ Determined from Cluster Calculations for the Spin Dimers $(CuCl_4^{2-})_2$ without the Intervening $Cs^+$ Ions

| | band calculations for $A_2CuCl_4$ | | | | cluster calculations |
|---|---|---|---|---|---|
| | A = Cs | A = Rb | A = K | A = Na | |
| $J_1/k_B$ | −8.5 | −14.0 | −16.6 | −21.2 | −36.2 |
| $J_2/k_B$ | −4.8 | −4.8 | −4.8 | −4.5 | −4.3 |
| $J_3/k_B$ | 0.0 | −3.6 | −6.2 | −12.6 | −12.8 |
| $J_4/k_B$ | +0.3 | +0.2 | +0.3 | +0.7 | 0.3 |

functional[8] and the 6-31++G(d, p) basis set. In these calculations, the $Cs^+$ ions present between the two $CuCl_4^{2-}$ ions are neglected. In these calculations, the spin exchange parameters $J$ is related to the energies of the high-spin (HS) and broken-symmetry (BS) states of the spin dimer ($E_{HS}$ and $E_{BS}$, respectively) as[9]

$$J = 2(E_{BS} - E_{HS}) \quad (1)$$

The $J_i/k_B$ values (in units of K) determined from these calculations on the basis of the RT crystal structure of $Cs_2CuCl_4$[3a] are summarized in the last column of Table 2, which shows that $J_1$ and $J_3$ are the two dominating AFM interactions, as anticipated from their short Cl···Cl contact distances (Table 1a). The frustrated two-leg spin ladder model (Figure 1d) resulting from $J_1$ and $J_3$ is not in agreement with experiment. This failure of the cluster calculations is due most likely to the neglect of the $Cs^+$ ions. Note that the arrangement of the $CuCl_4^{2-}$ and $Cs^+$ ions has pseudo mirror-plane symmetry in the SSE path $J_1$, pseudo inversion symmetry in $J_3$, but no symmetry in $J_2$ and $J_4$. The effect of the $Cs^+$ ions on the SSE interactions should depend on the geometrical arrangement of the $CuCl_4^{2-}$ and $Cs^+$ ions,

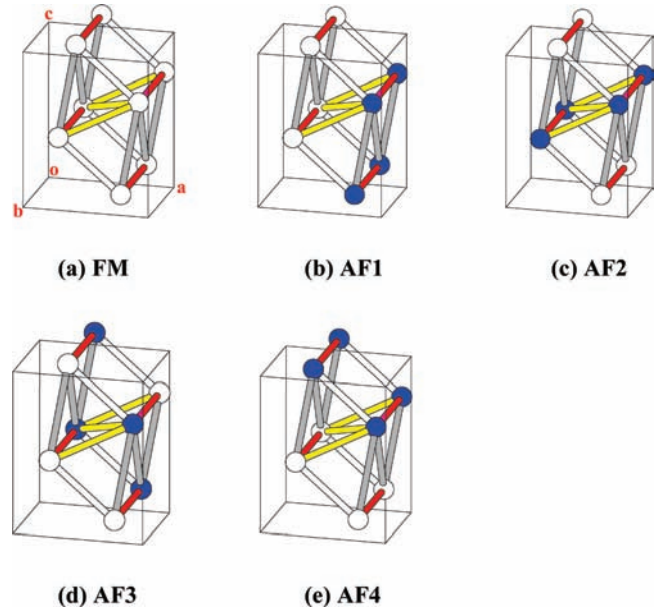


**Figure 3.** Five ordered spin states of $Cs_2CuCl_4$ employed to extract the spin exchange parameters $J_1-J_4$. The filled and empty circles represent up-spin and down-spin, respectively.

because the dominance of $J_1$ and $J_3$ in the absence of the $Cs^+$ ions should be converted into that of $J_1$ and $J_2$ in the presence of the $Cs^+$ ions.

## 3. Spin Exchange Parameters from Electronic Band Structure Calculations

To confirm the implication of the previous section, we carried out first principles DFT electronic band structure calculations for the RT crystal structure of $Cs_2CuCl_4$ by employing the frozen-core projector augmented wave method encoded in the Vienna ab initio simulation package (VASP)[12] with the generalized-gradient approximation (GGA) for the exchange-correlation functional,[13] the plane-wave cutoff energy of 400 eV, 96 k-points for the irreducible Brillouin zone, and the threshold of $10^{-6}$ eV for the self-consistent-field convergence of the total electronic energy. To properly describe the strong electron correlation of the Cu 3d states, we employ the GGA plus on-site repulsion U (GGA+U) method.[14] To evaluate the SSE parameters $J_1-J_4$ by GGA+U calculations using the VASP, we calculate the energies of the five ordered spin states $Cs_2CuCl_4$ shown in Figure 3. The relative energies of these states obtained for the RT structure of $Cs_2CuCl_4$ with $U$ = 2, 4, and 6 eV on Cu are summarized in Table 3a.

The energies of the five ordered spin states FM, AF1, AF2, AF3, and AF4 can be expressed in terms of the spin Hamiltonian,

$$\hat{H} = -\sum_{i<j} J_{ij}\hat{S}_i\cdot\hat{S}_j \quad (2)$$

(8) (a) Beck, A. D. *J. Chem. Phys.* **1993**, *98*, 5648. (b) Lee, C.; Yang, W.; Parr, R. G. *Phys. Rev. A* **1988**, *37*, 785.
(9) (a) Noodleman, L. *J. Chem. Phys.* **1981**, *74*, 5737. (b) Dai, D.; Whangbo, M.-H. *J. Chem. Phys.* **2003**, *118*, 29.
(10) Blöchl, P. E. *Phys. Rev. B* **1994**, *50*, 17953.
(11) Kresse, G.; Joubert, D. *Phys. Rev. B* **1999**, *59*, 1758.
(12) Kresse, G.; Furthmüller, J. *Phys. Rev. B* **1996**, *54*, 11169.
(13) Perdew, J. P.; Burke, K.; Ernzerhof, M. *Phys. Rev. Lett.* **1996**, *77*, 3865.
(14) Dudarev, S. L.; Botton, G. A.; Savrasov, S. Y.; Humphreys, C. J.; Sutton, A. P. *Phys. Rev. B* **1998**, *57*, 1505.

where $\hat{S}_i$ and $\hat{S}_j$ are the spin operators at the spin sites $i$ and $j$, respectively, and $J_{ij}$ (= $J_1$, $J_2$, $J_3$, $J_4$) is the SSE parameter between the sites $i$ and $j$. Then, by applying the energy expressions obtained for spin dimers with $N$ unpaired spins per spin site (in the present case, $N = 1$),[9b] the energies (per four formula units) for the five spin states of $Cs_2CuCl_4$ are written as

$$E_{FM} = (-4J_1 - 8J_2 - 4J_3 - 4J_4)N^2/4$$
$$E_{AFI} = (-4J_1 - 8J_2 + 4J_3 + 4J_4)N^2/4$$
$$E_{AF2} = (-4J_1 + 8J_2 - 4J_3 + 4J_4)N^2/4$$
$$E_{AF3} = (+4J_1 - 4J_4)N^2/4$$
$$E_{AF4} = (-4J_1 + 8J_2 + 4J_3 - 4J_4)N^2/4 \quad (3)$$

Therefore, by mapping the energy differences of the five states obtained from the GGA+U calculations onto the corresponding energy differences obtained from the spin Hamiltonian,[6,9b] we obtain the spin exchange parameters listed in Table 4a. For $U$ = 2, 4, and 6 eV, our GGA+U calculations show that $J_1$ and $J_2$ are the two dominant AFM interactions leading to the 2D triangular AFM spin−lattice (Figure 1c) in agreement experiment. Experimentally, $J_1/k_B = -4.34$ K, and $J_2/k_B = -1.48$ K,[2,4] so that our calculations overestimated the spin exchange parameters by a factor of ~3. This is not surprising because DFT calculations with the GGA[13] for the exchange-correlation functional tend to overestimate spin exchange parameters by a factor of up to ~4.[15] The experimental $J_2/J_1$ ratio of 0.34[4] is best reproduced by $U$ = 6 eV (i.e., $J_2/J_1$ = 0.56, 0.63, 0.86 for $U$ = 6, 4, and 2 eV, respectively). Thus, our discussion hereafter will be based on results from the use of $U$ = 6 eV.

**Table 3.** Relative Energies (in meV per Four Formula Units) of the Five Ordered Spin States of the RT and LT Crystal Structures of $Cs_2CuCl_4$ Obtained from the GGA+U Calculations As a Function of $U$

| | $U$ = 2 eV | $U$ = 4 eV | $U$ = 6 eV |
|---|---|---|---|
| | (a) RT Structure (ref 3a) | | |
| FM | 0.00 | 0.00 | 0.00 |
| AF1 | 0.20 | 0.09 | 0.05 |
| AF2 | −2.70 | −2.12 | −1.59 |
| AF3 | −3.09 | −2.86 | −2.30 |
| AF4 | −2.85 | −2.22 | −1.65 |
| | (b) Experimental (ref 3b) and Calculated LT Structures [a] | | |
| FM | 0.00 (0.00) | 0.00 (0.00) | 0.00 (0.00) |
| AF1 | +0.02 (−0.34) | −0.02 (−0.25) | −0.03 (−0.19) |
| AF2 | +0.37 (−2.49) | +0.11 (−1.87) | +0.02 (−1.39) |
| AF3 | +0.17 (−6.31) | −0.33 (−5.29) | −0.42 (−4.12) |
| AF4 | +0.12 (−3.03) | −0.05 (−2.26) | −0.09 (−1.67) |

[a] The relative energies for the calculated LT crystal structure (see Supporting Information, Table S1) are given in parentheses.

**Table 4.** Spin Exchange Parameters $J_1/k_B - J_4/k_B$ (in K) Determined for the RT and LT Structures of $Cs_2CuCl_4$ from the GGA+U Calculations As a Function of $U$

| | $U$ = 2 eV | $U$ = 4 eV | $U$ = 6 eV |
|---|---|---|---|
| | (a) RT Structure (ref 3a) | | |
| $J_1/k_B$ | −9.7 | −10.1 | −8.5 |
| $J_2/k_B$ | −8.3 | −6.4 | −4.8 |
| $J_3/k_B$ | +0.1 | 0.0 | 0.0 |
| $J_4/k_B$ | +1.0 | +0.5 | +0.3 |
| | (b) Experimental (ref 3b) and Calculated LT Structures [a] | | |
| $J_1/k_B$ | +0.6 (−27.8) | −1.8 (−24.1) | −2.2 (−19.1) |
| $J_2/k_B$ | +0.7 (−7.5) | +0.1 (−5.6) | −0.1 (−4.2) |
| $J_3/k_B$ | −0.7 (−2.6) | −0.5 (−1.9) | −0.4 (−1.4) |
| $J_4/k_B$ | +0.8 (+0.6) | +0.4 (+0.4) | +0.2 (+0.3) |

[a] The relative energies for the calculated LT crystal structure (see Supporting Information, Table S1) are given in parentheses.

## 4. Discussion

**4.1. Symmetry-Dependent Participation of Cs 6p Orbitals in Spin Exchange.** It is interesting to compare the spin exchange parameters $J_1-J_4$ of $Cs_2CuCl_4$ obtained from the cluster calculations neglecting the $Cs^+$ ions with those determined from the band structure calculations including the $Cs^+$ ions. Table 2 shows that the inclusion of the $Cs^+$ ions significantly weakens $J_1$ and $J_3$, but does not much affect $J_2$ and $J_4$. To account for this selective participation of the $Cs^+$ ions into the spin exchange interactions, we consider the symmetry of the arrangement of the $CuCl_4^{2-}$ and $Cs^+$ ions associated with each SSE path. As already noted (Figure 2), the arrangement has pseudo mirror-plane symmetry in $J_1$, pseudo inversion symmetry in $J_3$, but no symmetry in $J_2$ and $J_4$. From the viewpoint of orbital interactions,[6] the strength of the SSE interaction between two $CuCl_4^{2-}$ ions is proportional to $(\Delta e)^2$, where $\Delta e$ is the energy split between the two magnetic orbitals, $\Psi_+$ and $\Psi_-$, of the spin dimer $(CuCl_4^{2-})_2$. As depicted in Figure 4a,b for $J_1$, $\Psi_+$ and $\Psi_-$ are given by the bonding and antibonding combinations of the magnetic orbitals of the constituent $CuCl_4^{2-}$ ions.[16] By symmetry, the magnetic orbital $\Psi_-$ can make bonding interaction with the 6p orbitals of the intervening $Cs^+$ ions to reduce the $\Delta e$ value (Figure 4c). This reasoning assumed that the energy lowering of $\Psi_-$ by the 6p orbitals of the $Cs^+$ ions is much stronger than that of $\Psi_+$ by the 6s orbitals of the $Cs^+$ ions. If this is true, the plot of density of states calculated for $Cs_2CuCl_4$ should show that, in the occupied energy region, the Cs 6p orbital contribution is much stronger than the Cs 6s orbital contribution. This is indeed the case, as shown in Figure 5.

There are two factors that affect the lowering of the $\Psi_-$ orbital by the Cs 6p orbitals; one is the symmetry of the arrangement of the $CuCl_4^{2-}$ and $Cs^+$ ions. Only when this arrangement is symmetrical as found for the SSE paths $J_1$ and $J_3$ (Figure 2) can $\Psi_-$ make bonding interaction with the 6p orbitals of the $Cs^+$ ions. The other factor is the spatial extension of the Cs 6p orbital, which appears ideal for its overlap with $\Psi_-$ in the SSE paths $J_1$ and $J_3$. To verify this implication, we construct the hypothetical compounds $A_2CuCl_4$ (A = Rb, K, Na) by replacing the Cs atoms of $Cs_2CuCl_4$ with smaller alkali atoms Rb, K, or Na, without

(15) (a) Dai, D.; Whangbo, M.-H. *J. Chem. Phys.* **2001**, *114*, 2887. (b) Dai, D.; Koo, H.-J.; Whangbo, M.-H. *J. Solid State Chem.* **2003**, *175*, 341. (c) Dai, D.; Whangbo, M.-H.; Koo, H.-J.; Rocquefelte, X.; Jobic, S.; Villesuzanne, A. *Inorg. Chem.* **2005**, *44*, 2407. (d) Grau-Crespo, R.; de Leeuw, N. H.; Catlow, C. R. *J. Mater. Chem.* **2003**, *13*, 2848. (e) Koo, H.-J.; Whangbo, M.-H. *Inorg. Chem.* **2008**, *47*, 128. (f) Koo, H.-J.; Whangbo, M.-H. *Inorg. Chem.* **2008**, *47*, 4779.

(16) The orbital plots were made from extended Hückel tight binding calculations using the SAMOA program (http://chvamw.chem.ncsu.edu).

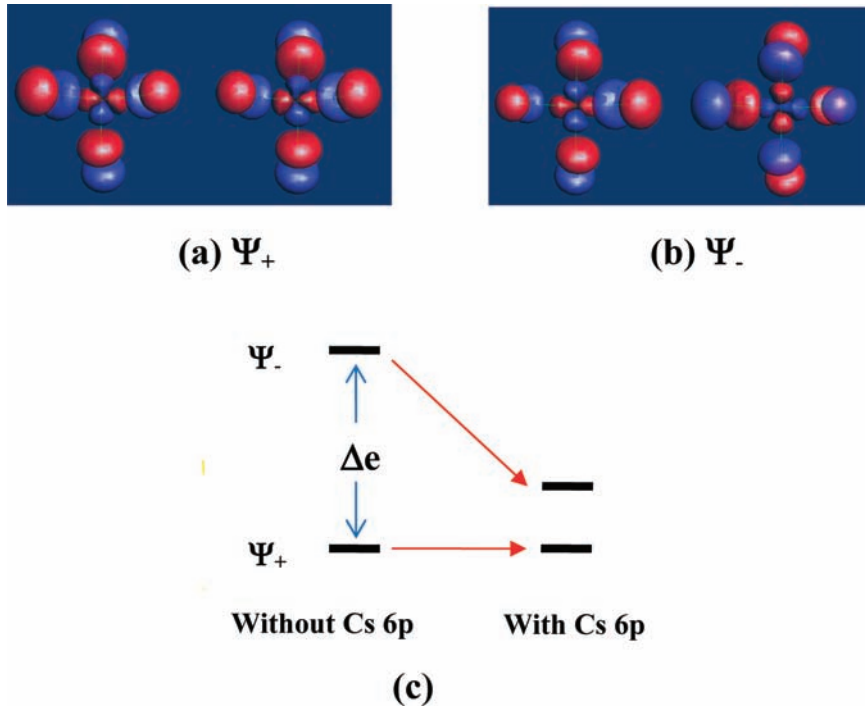


**Figure 4.** (a, b) Magnetic orbitals $\Psi_+$ and $\Psi_-$ and their energy split $\Delta e$ in the spin dimer unit $(CuCl_4^{2-})_2$ associated with the spin exchange path $J_1$. (c) Lowering of the $\Psi_-$ level by the 6p orbitals of the intervening $Cs^+$ ions.

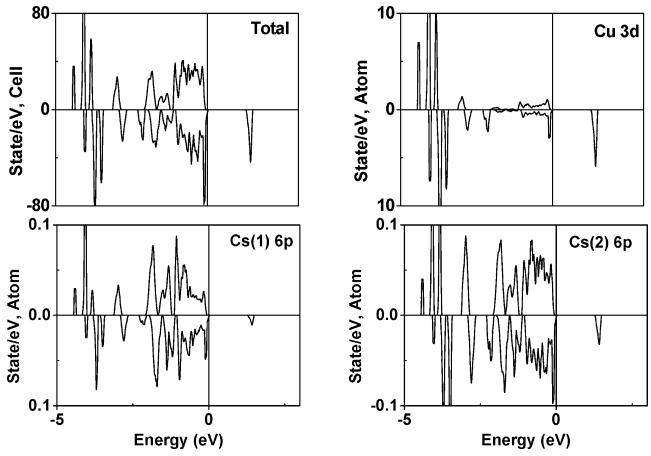


**Figure 5.** Plots of the total and partial density of states determined for $Cs_2CuCl_4$ from the GGA+U calculations with $U = 6$ eV. The upper and the lower panels of each diagram represent the up-spin and down-spin band structures, respectively. There are two nonequivalent Cs atoms, Cs(1) and Cs(2), in $Cs_2CuCl_4$. The Cs 6s orbital contribution is lower in magnitude than the Cs 6p orbital contribution by an order of magnitude, and hence is not shown.

relaxing the resulting structures. The spatial extension of the *n*p ($n = 6-3$) orbital of A (A = Cs, Rb, K, Na) decreases gradually with decreasing *n*. Therefore, the reduction of $\Delta e$ in the SSE path $J_1$ or $J_3$ would decrease in the order, Cs > Rb > K > Na. Consequently, the strength of $J_1$ or $J_3$ should increase in the order Cs < Rb < K < Na. This prediction is confirmed by the SSE parameters determined for the RT structures of $A_2CuCl_4$ (A = Cs, Rb, K, Na) on the basis of our GGA+U calculations (with $U = 6$ eV) (Table 2). Note that $J_3$ vanishes in $Cs_2CuCl_4$ because the interaction between the two $CuCl_4^{2-}$ ions through the intervening $Cs^+$ ions, which is strong because of their symmetrical arrangement, cancels out the direct interaction between the two $CuCl_4^{2-}$ ions. The strengths of $J_2$ and $J_4$ remain essentially constant for all alkali cations ($A^+ = Cs^+$, $Rb^+$, $K^+$, $Na^+$), because their $CuCl_4^{2-}$ ions and intervening $A^+$ ions have a low-symmetry arrangement.

It is clear from the above discussion that the 6p orbitals of $Cs^+$ ions can strongly affect spin exchange interactions. This finding is contrary to the usual belief that an alkaline metal element A acts simply as an electron donor with the resulting alkaline cation $A^+$ providing the electrostatic field. It has been reported[17] that the interchain spin exchange interactions of cyano-bridged $Ni^{2+}/M^{3+}$ (M = Cr, Fe, Co) chain complexes can be tuned by the size of the alkaline ion $A^+$. In this case, the interchain spin exchange increases in the order Li < K < Rb < Cs.[17] It is unclear whether this finding arises solely from the size of the alkaline ion or the orbitals of the alkaline ion are involved in the interchain spin exchange. An important related observation is that the 3d orbitals of the alkaline earth element Ca are essential in producing the interlayer band of $CaC_6$,[18] which is important for its superconductivity.

**4.2. LT Crystal Structure of $Cs_2CuCl_4$.** So far, our discussion was based on GGA+U calculations carried out for the RT crystal structure[3a] of $Cs_2CuCl_4$. The neutron scattering experiments[2,4] of $Cs_2CuCl_4$, which led to the 2D triangular AFM spin−lattice model, were carried out at very low temperatures (below 1 K).[2,4] Thus, it is of importance to check whether our conclusions based on the RT crystal structure remain valid if the LT crystal structure[3b] of $Cs_2CuCl_4$ is used for our analysis. We repeated our mapping analysis by using the experimental LT structure. However,

(17) Atanasov, M.; Comba, P.; Frster, S.; Linti, G.; Malcherek, T.; Miletich, R.; Prikhod'ko, A. I.; Wadepohl, H. *Inorg. Chem.* **2006**, *45*, 7722.
(18) Deng, S.; Simon, A.; Köhler, J. *Angew. Chem., Int. Ed.* **2008**, *47*, 6703.

the quality of this crystal structure is not high because it leads to unreasonably short Cs···Cl distances. As listed in Table 1b, some Cs···Cl distances are shorter than 3.48 Å, the sum of the ionic radii of $Cs^+$ and $Cl^-$ ions.[19] To remedy this undesirable situation, we optimized the atomic positions of $Cs_2CuCl_4$ on the basis of GGA+U calculations (with $U = 2$ eV) for the lowest-energy magnetic state (i.e., the AF3 state) of $Cs_2CuCl_4$ while keeping the cell parameters at those values found in the experimental structure.[3b] The optimized atomic positions are presented in the Supporting Information, Table S1. This calculated LT structure does not lead to unreasonably short Cs···Cl distances, as summarized in Table 1b.

Table 3b lists the relative energies of the five ordered spin states determined for the LT crystal structure of $Cs_2CuCl_4$ from GGA+U calculations, and Table 4b the spin exchange parameters resulting from the subsequent mapping analysis. Note that the 2D triangular AFM spin−lattice is not reproduced by the $J_1$−$J_4$ values determined from the experimental LT crystal structure but by those from the calculated LT crystal structure (with $J_2/J_1 = 0.27$, 0.23, and 0.22 for $U = 2$, 4, and 6 eV, respectively). Nevertheless, the calculated LT crystal structure is not quite perfect because the calculated $J_1$ is much stronger than the experimental value and because the calculated $J_3$ is not negligibly small. Thus, as has been observed,[6,20] use of accurate crystal structures is crucial in correctly determining the relative strengths of spin exchange interactions on the basis of electronic structure calculations.

(19) Shannon, R. D. *Acta Crystallogr. A* **1976**, *32*, 751.
(20) Koo, H.-J.; Whangbo, M.-H.; VerNooy, P. D.; Torardi, C. C.; Marshall, W. J. *Inorg. Chem.* **2002**, *41*, 4664.

## 5. Concluding Remarks

In summary, the 2D triangular antiferromagnetism of $Cs_2CuCl_4$ originates from the fact that the strength of the SSE interaction between adjacent $CuCl_4^{2-}$ ions is strongly reduced by the 6p orbitals of the intervening $Cs^+$ ions when the arrangement of the $CuCl_4^{2-}$ and $Cs^+$ ions has mirror-plane or inversion symmetry. This finding is contrary to the usual preconception that alkaline-metal and alkaline-earth elements act simply as electron donors without affecting the electronic structures of their hosts. Clearly, one needs to exercise caution in using this simplifying assumption, because the diffuse orbitals of these elements (e.g., 6p orbitals of Cs and 3d orbitals of Ca) can give rise to delicate changes in the electronic structures of the hosts hence affecting their magnetic and/or metallic properties.

**Acknowledgment.** This work was supported by the Office of Basic Energy Sciences, Division of Materials Sciences, U.S. Department of Energy, under Grant DE-FG02-86ER45259 and by the resources of the NERSC Center supported under Contract No. DE-AC02-05CH11231. J.H.K. and K.H.L. thank the support from the Korea Research Foundation Grant funded (MOEHRD, KRF-2007-612-C00036, and KRF-2007-313-C00332). M.H.W. thanks Dr. R. K. Kremer for an invaluable discussion.

**Supporting Information Available:** Further details are given in Table S1. This material is available free of charge via the Internet at http://pubs.acs.org.

IC802412X